Energetic-Ion-Driven Toroidal Alfvén Eigenmodes Observed in a Heliotron/Torsatron Plasma

M. Takechi,[1] K. Toi,[2] S. Takagi,[1] G. Matsunaga,[1] K. Ohkuni,[1] S. Ohdachi,[2] R. Akiyama,[2] D. S. Darrow,[3] A. Fujisawa,[2] M. Gotoh,[2] H. Idei,[2] H. Iguchi,[2] M. Isobe,[2] T. Kondo,[4] M. Kojima,[2] S. Kubo,[2] S. Lee,[2] T. Minami,[2] S. Morita,[2] K. Matsuoka,[2] S. Nishimura,[2] S. Okamura,[2] M. Osakabe,[2] M. Sasao,[2] M. Shimizu,[1] C. Takahashi,[2] K. Tanaka,[2] and Y. Yoshimura[2]

[1]*Department of Energy Engineering Science, Nagoya University, Nagoya 464-8601, Japan*
[2]*National Institute for Fusion Science, Toki 509-5292, Japan*
[3]*Princeton Plasma Physics Laboratory, Princeton, New Jersey 08543*
[4]*Department of Fusion Science, Graduate University for Advanced Studies, Toki 509-5292, Japan*

(Received 15 October 1998)

Toroidal Alfvén eigenmodes (TAEs) of low toroidal mode number, $n = 1$ and 2, are observed in neutral-beam-heated plasmas in the compact helical system heliotron/torsatron. The observed frequency is proportional to the computed TAE frequency and lies near the lower bound of the innermost TAE gap. The modes are excited only when the beam velocity exceeds about half the central Alfvén velocity and when the net plasma current induced by coinjected neutral beams is in the required range. The modes are localized in the plasma core region, between 0.2 and 0.6 of the plasma minor radius.

PACS numbers: 52.35.Bj, 52.35.Py, 52.35.Qz, 52.55.Hc

In a fusion reactor, it is predicted that Alfvén eigenmodes—such as the toroidal Alfvén eigenmodes (TAE) [1]—which are destabilized by the pressure gradient of energetic alpha particles with super-Alfvénic velocity, could expel the alpha particles before thermalization, and consequently lead to the quenching of ignition and damage to the first wall [2]. Accordingly, it is very important to clarify the excitation mechanism for TAEs, in order to be able to suppress TAE-induced alpha particle loss. In large tokamaks, the excitation of TAEs has been extensively studied by the use of energetic ions generated by neutral beam injection (NBI) [3–5] and ion cyclotron heating [4,6–8] and also by the use of alpha particles in a deuterium-tritium plasma [9].

TAE research is also important for helical systems, which are thought to be a promising alternative concept to the tokamak. The first observation of Alfvén eigenmodes in a helical system was achieved in W7-AS, where the so-called global Alfvén eigenmode (GAE) was excited by energetic beam ions [10]. Because of its very low magnetic shear configuration, the GAE was the most likely Alfvén eigenmode to be seen in the W7-AS stellarator. In contrast, a heliotron/torsatron is a helical system with moderate or high magnetic shear, comparable to that in a tokamak but with negative sign (where q is the safety factor and the radial derivative $q' < 0$). In the present work we investigate Alfvén eigenmodes in NBI-heated plasmas in the low-aspect-ratio compact helical system (CHS) heliotron/torsatron [11], which has major radius $R \approx 1$ m, average minor radius $\langle a \rangle \approx 0.2$ m, and toroidal and poloidal field period numbers $N = 8$ and $l = 2$, respectively. In CHS plasmas, the TAE frequency, estimated from the formula $f_{\mathrm{TAE}} = V_A/(4\pi R q)$ where V_A is the Alfvén velocity, increases rapidly towards the plasma edge because q decreases towards the edge—just the opposite to the tokamak configuration. As a result, the frequency of a TAE in the plasma core usually intersects the Alfvén continuum in the plasma edge where the magnetic shear is high, which can cause the corresponding TAE to be stabilized due to strong continuum damping [12,13]. However, it is possible for TAEs to be destabilized in this configuration if the magnetic shear in the plasma core is appreciably reduced by net plasma current I_p or finite plasma pressure. In this Letter, we describe the first observation of TAEs excited by energetic ions in CHS.

In CHS, a hydrogen beam was tangentially injected into a hydrogen plasma so that the spectrum of TAE fluctuations appeared in the frequency range higher than about 100 kHz and consequently was not contaminated by normal pressure-driven MHD modes whose frequency is typically less than 80 kHz. The toroidal field and line averaged electron density were scanned in the range of $B_t = 0.7$–1.5 T and $\overline{n}_e = (0.5$–$3) \times 10^{19}$ m^{-3}, respectively. The injection energy of the hydrogen beam E_b was varied from 28 to 40 keV. With this variation of plasma parameters, the ratio of the beam ion velocity V_b to the central Alfvén velocity $V_A(0)$ was scanned in the range $0.2 \leq V_b/V_A(0) \leq 1$. In these experiments the energetic beam-ion beta value was relatively high ($\langle \beta \rangle_{\mathrm{beam}} \approx 0.1\%$–$0.3\%$), being comparable to the bulk plasma beta value. Magnetic fluctuations near the last closed flux surface (LCFS) were measured with a movable magnetic probe array, by means of which magnetic fluctuations at six radial positions could be simultaneously obtained [14]. In CHS, because five magnetic probes for measuring the toroidal mode number n are arranged only every 45° in the toroidal direction, we can only measure n in the combination $n + 8k$ (for integer k). The radial profile for the magnetic fluctuations as obtained from the movable probe array gives information

 0031-9007/99/83(2)/312(4)$15.00

about the dominant poloidal mode number m, being assumed that the probe array is placed in the scrape-off plasma without any current perturbations due to the magnetic fluctuations. Using both the probe array and Mirnov probes, we successfully determined n of the TAE oscillations [14]. The TAE radial mode structure was obtained from a 20-channel soft x-ray detector array (SX array) with fast time response (up to 200 kHz) [15] and from a heavy ion beam probe (HIBP) [16].

Figure 1 shows the typical time evolution of the magnetic fluctuations in an NBI-heated hydrogen plasma in CHS for which the magnetic axis position of the vacuum field is $R_{ax} = 0.95$ m, where $B_t = 1.2$ T and $E_b = 39$ keV. Two coherent modes are clearly identified, having very narrow spectral width (≤ 1 kHz) and fluctuation level $b_\theta \approx 1 \times 10^{-6}$ T at the LCFS. The toroidal mode number is $n = 1$ for the lower frequency mode, and $n = 2$ for the higher one. The dominant poloidal mode number is $m \approx 2$ for the $n = 1$ mode and $m \approx 4$ for the $n = 2$ mode. Two solid curves in Fig. 1(a) indicate TAE frequencies corresponding to the innermost TAE gap (i.e., nearest the magnetic axis) $f^H_{\mathrm{TAE}}(0)$, which were estimated for a pure hydrogen plasma with the use of $n_e(0)$ and q at the gap position [i.e., $q = (m + 1/2)/n$]. The lower curve shows $f^H_{\mathrm{TAE}}(0)$ for the $n = 1$ mode related to poloidal mode coupling between the $m = 2$ and $m = 3$ harmonics, and the upper curve is $f^H_{\mathrm{TAE}}(0)$ for the $n = 2$ mode related to the $m = 4$ and $m = 5$ coupling. As seen from the figure, both of the observed mode frequencies f_{obs} evolve in time, proportional to $f^H_{\mathrm{TAE}}(0)$, although f_{obs} are lower than $f^H_{\mathrm{TAE}}(0)$ by about 30%. Figure 2 shows the dependence of f_{obs} for various B_t and $\overline{n}_e$, plotted versus $f^H_{\mathrm{TAE}}(0)$. This figure clearly indicates that f_{obs} for the magnetic fluctuations scales well with $f^H_{\mathrm{TAE}}(0)$, but is about 30% lower than $f^H_{\mathrm{TAE}}(0)$, just as in Fig. 1. These results in Figs. 1 and 2 suggest that these modes are TAEs excited by injected energetic beam ions. The difference between f_{obs} and $f^H_{\mathrm{TAE}}(0)$ can be well explained by the presence of impurity ions and the TAE gap width, as discussed later. Note that the effect of toroidal plasma rotation on f_{obs} is very small, that is, ~3 kHz for $n = 1$ and ~6 kHz for $n = 2$, respectively, since the rotation of about 20 km/s is predicted at the plasma center [17].

Calculation of the TAE gap structure in the three-dimensional configuration of CHS is fairly complicated and at present is not available for our experiments. Therefore, a simple calculation of the shear Alfvén continua in a cylindrical configuration is here employed to predict the frequency range and radial location of the TAE gap. The TAE gap structure is calculated by a simple dispersion relation for a large-aspect-ratio tokamak equilibrium [1]. Here, the expression for the TAE (full) gap width includes the effect of helical field ripple as $2\Delta f \approx 2(\varepsilon_t + \varepsilon_h + \Delta')f_{\mathrm{TAE}}$, where ε_h is the helical ripple, ε_t is the toroidal ripple ($\approx\langle r\rangle/R$), and Δ' is the radial derivative of the Shafranov shift. Note that in the region of $\rho \leq 0.7$ (ρ: the normalized minor radius to the plasma radius), the width $2\Delta f$ is dominantly determined by the term of $(\varepsilon_t + \Delta')$. The q profile is derived from the sum of the rotational transform $(1/q)$ due to I_p and the external rotational transform in a three-dimensional current-free equilibrium with an average total beta of 0.2%, where the current density profile is assumed to be the shape $j_\varphi = j_0(1 - \rho^2)^\lambda$. The peaking parameter λ was chosen in the plausible range $1 \leq \lambda \leq 2$. Figure 3(a) shows a typical example of the uncoupled shear Alfvén spectra and TAE gaps calculated by the above-mentioned simple equation for the $n = 1$ mode observed at 120 ms in the shot of Fig. 1, where the measured n_e profile and the calculated $1/q$ profile (solid curve) shown in Fig. 3(c) were employed and $\lambda = 1.5$ was assumed. Moreover, the plasma mass density was enhanced by a factor of 1.4 in order to simulate the presence of fully ionized carbon and oxygen (the effective plasma charge $Z_{\mathrm{eff}} = 2-3$). The $1/q$ profile(dotted curve) in a low I_p case without observation of TAEs is also shown in Fig. 3(c). As shown in Fig. 3(a), the observed frequency of $n = 1$ mode lies near the lower bound of the innermost TAE gap. The similar feature was also found for the $n = 2$ mode, as shown in Fig. 3(b).

The internal structure of TAEs was measured with the SX array. However, the soft X-ray fluctuation level for TAEs is too low to obtain the radial profile of the fluctuation intensity because of the relatively low electron

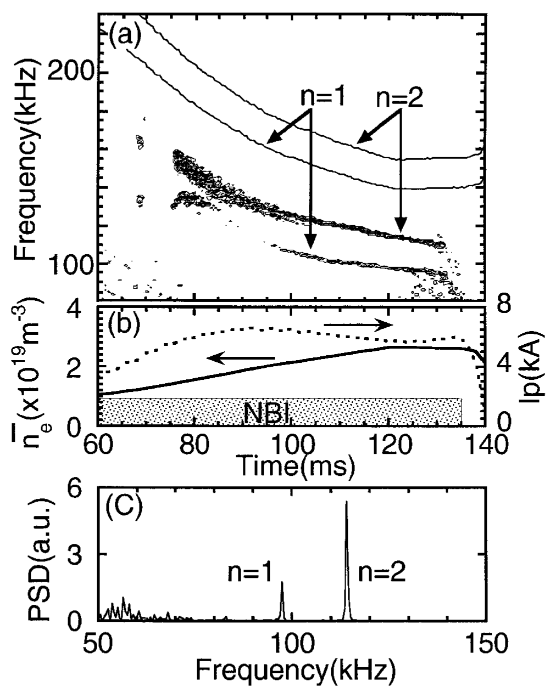

FIG. 1. (a) Contour plot of magnetic fluctuation intensity vs frequency and time for the NBI-heated plasma shown in (b). Also shown are the calculated TAE frequencies at the plasma center for a pure hydrogen plasma. (b) Time evolution of the electron density and the net plasma current in an NBI-heated plasma, with $B_t = 1.2$ T. (c) Spectral power density for the magnetic fluctuations ($t = 120-122$ ms) in (a).

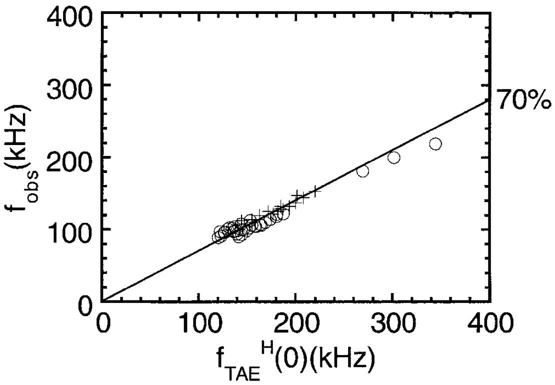

FIG. 2. Comparison of the observed TAE frequency, f_{obs}, with the TAE frequency calculated at the plasma center $f^{H}_{\mathrm{TAE}}(0)$, for a pure hydrogen plasma, with the q value estimated as $q = (m + 1/2)/n$. Open circle denotes the $n = 1$ mode, and plus sign indicates the $n = 2$ mode. The solid line corresponds to 70% of $f^{H}_{\mathrm{TAE}}(0)$.

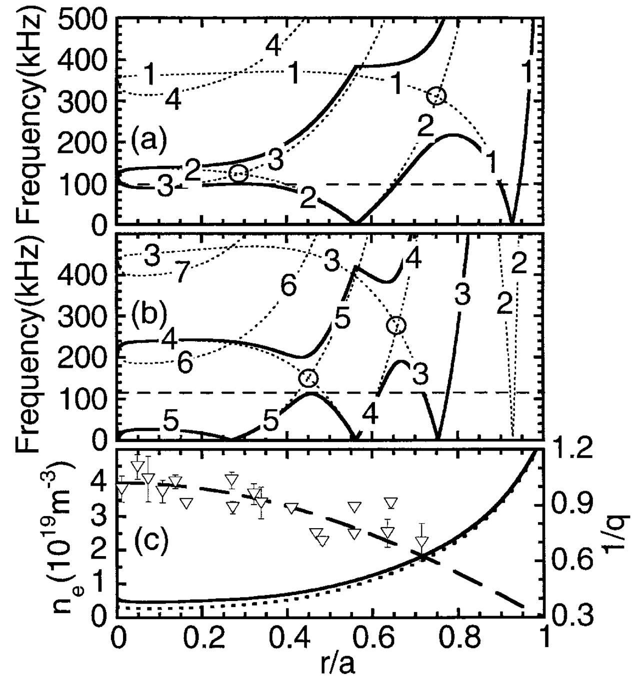

FIG. 3. (a) Shear Alfvén continua in the cylindrical geometry (dotted curve) for the $n = 1$ mode, at 120 ms of Fig. 1, where the presence of impurity ions is taken into account. The Alfvén continua are labeled by the respective m. Open circles indicate the TAE gaps, and the thick curve shows the calculated TAE gap. The horizontal broken line indicates the observed frequency. (b) Results for the $n = 2$ mode. (c) The radial profiles for the measured electron density and the calculated rotational transform $1/q$ (solid curve) where the net current effect is included. The $1/q$ profile in the case without observation of TAEs is also shown by the dotted curve.

temperature ($T_{e0} \leq 0.3$ keV). For this reason, the coherence γ between the soft-x-ray signal of each channel and the magnetic probe signal was calculated in the TAE frequency range. Figure 4(a) shows the radial profiles of γ for the $n = 1$ and $n = 2$ TAEs observed in the shot of Fig. 1, for which $R_{\mathrm{ax}} = 0.95$ m. This figure suggests that the high γ region is localized within $\rho \approx 0.6$, where $\gamma \approx 0.3$ for noise. Note that the high γ observed around the plasma center is caused by the integral effect of soft x-ray emission along the line of sight. Therefore, the TAEs are estimated to be localized around $\rho \approx 0.2$–0.6. TAEs with $n = 1$ are observed also in inward shifted plasmas with $R_{\mathrm{ax}} = 0.92$ m, where HIBP data are available. Figure 4(b) shows the radial profile of the plasma potential fluctuations and of γ, where the potential fluctuations are normalized to the TAE magnetic fluctuations b_θ in respective shots because HIBP data are obtained shot by shot. This figure clearly shows mode localization at $\rho \approx 0.2$–0.6. These results are consistent with the results shown in Fig. 3. The observed TAEs exhibit ballooning nature, as can be seen in Fig. 4.

In CHS, when the velocity of tangentially injected beams V_b exceeds about half the central Alfvén velocity $V_A(0)$, TAE fluctuations are excited well above the noise level of a magnetic probe. This seems to suggest the sideband excitation in which passing beam ions resonate with the TAEs when $V_b/V_A = 1/3$ [18]. As was mentioned earlier, when the magnetic shear in the plasma core is appreciably reduced by I_p induced by co-NBI, it is possible for TAEs localized in the plasma core to be more unstable [19]. We have tested this possibility by varying I_p. In the configuration with $R_{\mathrm{ax}} = 0.95$ m, I_p required to excite TAEs is in the range of 0.5–4.5 kA when $B_t = 0.9$ T. The required I_p increases as B_t increases: e.g., the required I_p becomes 3–6 kA when $B_t = 1.2$ T. The upper bound of I_p is determined by elimination of the relevant TAE gap. These results suggest that low magnetic shear created in the core plasma in this way facilitates the excitation of TAEs in CHS.

In Fig. 3 we have taken ε_h into account in a simplistic manner, by merely adding it to ε_t. However, three-dimensional configurations such as CHS have another important effect, namely, toroidal mode coupling [20]. In this case the n-mode family which consists of many harmonics with the different toroidal mode number $n' = \pm(n - Nk)$ takes the place of mode coupling and generates densely packed TAE gaps, where the toroidal field period number $N = 8$ in CHS and $k = 0, \pm 1, \pm 2, \ldots$. This leads to formation of the envelope of the TAE gaps calculated in the axisymmetric configuration. Although thus modified Alfvén spectrum might bring about appreciable continuum damping, the TAE gap structure shown in Fig. 3 is still useful to predict the possible frequency and radial extent of TAEs. Detailed numerical calculation in the three-dimensional configuration is required to estimate enhancement of continuum damping due to the spectrum modification and is left for a future study.

As noted previously, a certain I_p is required to excite TAEs in CHS. If the NBI-induced current has a highly peaked profile, this considerably modifies the q profile in the plasma core, such that the innermost $n = 1$ TAE

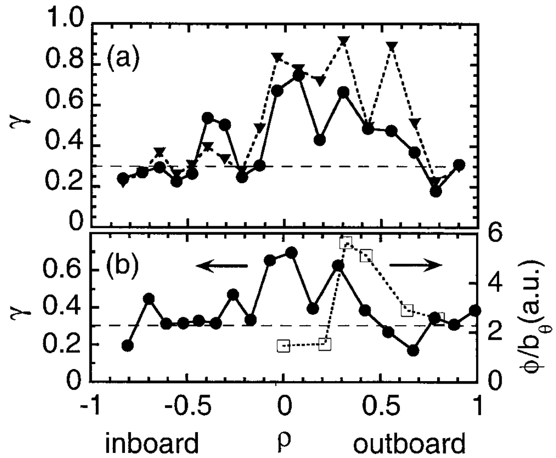

FIG. 4. (a) Radial profiles for the coherence γ between the soft-x-ray signal of each channel and the magnetic probe signal, for the modes with $n = 1$ (solid circles) and $n = 2$ (solid triangles) observed in the shot of Fig. 1, with $R_{\rm ax} = 0.95$ m. The coherence level for noise is $\gamma \sim 0.3$ (horizontal line). (b) Radial profiles of γ (solid circles) and the potential fluctuations measured by HIBP (open squares) in the plasma with $R_{\rm ax} = 0.92$ m. The potential fluctuations are normalized to the TAE level b_θ in respective shots.

gap can be eliminated. In this situation, GAEs might be destabilized near the plasma center. However, as shown in Fig. 1, the observed $m \approx 2$ and $n = 1$ are different from those of the predicted GAE ($m = 3$ and $n = 1$). Therefore, GAEs are excluded in the present experiments. Helicity-induced Alfvén eigenmodes [21] are also excluded, because their frequencies are much higher than the experimental data.

On the initial TAE campaign in CHS, the TAE with bursting amplitude modulation was observed in a few shots with high NBI power [22]. However, the mode numbers and internal structure could not be derived due to very small data base. The bursting TAE is a very important issue to be clarified in the future, from the viewpoints of the related energetic ion loss. The TAEs shown in this Letter, however, indicate no enhanced ion loss in the signals of a newly installed escaping ion probe (EIP) [23]. This might be due to the fluctuation amplitude ($b_\theta/B_t < 10^{-5}$ at LCFS), the limited space coverage of EIP, or redistribution of energetic ion profile without prompt loss, and so far is not clearly understood.

In summary, TAEs have been identified for the first time in the CHS heliotron/torsatron in NBI-heated plasmas. The modes are observed only when the beam velocity exceeds about half the central Alfvén velocity and when the net plasma current induced by co-NBI is in the required range to minimize the central magnetic shear and retain the TAE gap, depending on the toroidal magnetic field. The observed TAEs are localized in the plasma core, which has fairly low magnetic shear due to the net plasma current. Investigations on detailed comparison of experimental data with the detailed three-dimensional analysis, the nonlinear evolution of TAEs, and the effect on energetic ion loss are left as future important issues on TAEs in helical plasmas.

The authors thank the other members of the toroidal experimental group and also Professor H. Yamada for experimental support. Fruitful discussions with Professor N. Nakajima, Professor Y. Nakamura, Professor M. Wakatani, and Professor J. W. Van Dam are gratefully acknowledged.

[1] C. Z. Cheng and M. S. Chance, Phys. Fluids **29**, 3695 (1986).
[2] G. Y. Fu and J. W. Van Dam, Phys. Fluids B **1**, 1949 (1989).
[3] K. L. Wong *et al.*, Phys. Fluids B **4**, 2122 (1992).
[4] S. Ali-Arshad and D. J. Cambell, Plasma Phys. Controlled Fusion **37**, 715 (1995).
[5] W. W. Heidbrink *et al.*, Nucl. Fusion **31**, 1635 (1991).
[6] J. R. Wilson *et al.*, in *Plasma Physics and Controlled Nuclear Fusion Research 1992: Proceedings of the 14th IAEA Conference Würzburg* (IAEA, Vienna, 1993), Vol. 1, p. 661.
[7] H. Kimura *et al.*, Phys. Lett. A **86**, 199 (1995).
[8] M. Saigusa *et al.*, in *Plasma Physics and Controlled Nuclear Fusion Research 1994: Proceedings of the 15th IAEA Conference Seville* (IAEA, Vienna, 1995), Vol. 1, p. 453.
[9] R. Nazikian *et al.*, Phys. Rev. Lett. **78**, 2976 (1997).
[10] A. Weller *et al.*, Phys. Rev. Lett. **72**, 1220 (1994).
[11] K. Matsuoka *et al.*, in *Plasma Physics and Controlled Nuclear Fusion Research 1988: Proceedings of the 12th IAEA Conference Nice, 1988* (IAEA, Vienna, 1989), Vol. 2, p. 411.
[12] M. N. Rosenbluth *et al.*, Phys. Rev. Lett. **68**, 596 (1992).
[13] A. D. Turnbull *et al.*, Phys. Fluids B **5**, 2546 (1993).
[14] M. Takechi and K. Toi, Rev. Sci. Instrum. **70**, 442 (1999).
[15] S. Ohdachi *et al.*, in *Proceedings of the 24th EPS Conference on Plasma Physics and Controlled Fusion, Berchtesgaden, 1997* (Plasma Science and Fusion Center, MIT, Cambridge, MA, 1997), Vol. 21A, Part II, p. 813.
[16] A. Fujisawa *et al.*, Rev. Sci. Instrum. **67**, 3099 (1996).
[17] K. Ida *et al.*, Phys. Rev. Lett. **67**, 58 (1991).
[18] H. Biglari *et al.*, Phys. Fluids B **4**, 2385 (1992).
[19] G. Y. Fu *et al.*, Phys. Rev. Lett. **75**, 2336 (1995).
[20] N. Nakajima and Y. Nakamura (private communication).
[21] N. Nakajima *et al.*, Phys. Fluids B **4**, 1115 (1992).
[22] K. Toi *et al.*, J. Plasma Fusion Res. **1**, 267 (1998).
[23] D. S. Darrow *et al.*, J. Plasma Fusion Res. **1**, 362 (1998).